

Parameter optimization and economic analysis of a single-effect mechanical vapor compression (MVC) distillation system

Cong Liu*, Mingshu Bi, Guangrui Cui

School of Chemical Machinery, Dalian University of Technology, 116023, China, emails: costaliugame@main.dlut.edu.cn (C. Liu), bimsh@dlut.edu.cn (M.S. Bi), cuiguangrui.xuexi@foxmail.com (G.R. Cui)

Received 20 September 2019; Accepted 7 May 2020

ABSTRACT

The current study is focused on the parameter optimization and economic analysis of a single-effect mechanical vapor compression (MVC) distillation system design. For this purpose, the effect of the parameters (seawater temperature, seawater flow rate, feed seawater temperature, and feed seawater and saturation temperature difference) on the MVC system performance (recovery ratio) is first discussed to obtain the optimal parameters. Second, an economic analysis is conducted to compare the simplified cost of water (SCOW) values at various plant capacities and recovery ratios. The results indicate that the recovery ratio grows with the increase in feed seawater temperature and the temperature difference between the feed temperature and saturation temperature. The variation in seawater temperature only affects the preheater area, not the evaporator performance. With increasing seawater temperature, the preheater area decreases. The economic analysis indicates that with increased feed seawater flow rate and recovery ratio, SCOW shows a decreasing trend from 2.37 to 2.03 (\$/ton). With an increased feed seawater flow rate and recovery ratio, SCOW also decreased.

Keywords: Mechanical vapor compression; Single-stage; Python language; Parameters optimization; Economic analysis

1. Introduction

As a kind of vital resource for human development, water is an abundant element on earth, but most water is salty (97.5%). Freshwater has disappeared quickly with overexploitation and pollution. Many countries have realized the importance of water resources and are trying to find all kinds of methods to solve the problem.

Desalination presents a solution to overcome freshwater scarcity [1], especially for countries and regions that lack freshwater, such as North America, North Africa, the Middle East, and so on. There are different technologies for water desalination. Membrane desalination and thermal desalination are the most common technologies [2].

Reverse osmosis (RO) is the applicable membrane desalination process. It removes solid particles from feedwater using pressure with the help of the membrane. The RO

method has several disadvantages, including high operation costs, strict requirements for wastewater quality, and the equipment is easily destroyed. Thermal desalination is considered to be one of the oldest desalination methods. It relies on the available heat source to produce freshwater via evaporation. Thermal desalination technology can be involved in several categories such as multi-stage flash (MSF), multi-effect evaporation (MEE), thermal vapor compression, and mechanical vapor compression (MVC) [2]. In the MSF process, seawater is first heated within tubes by convection and then the vapor is initiated by flashing as it streams in each stage of reduced pressure. In the other three processes, vapor originates from the falling film of seawater that is brought in contact with the heat transfer surface [2]. Compared with the MSF process, the other processes have several advantages including fewer manufacturing requirements, sample pre-treatment, less start-up

* Corresponding author.

time, and lower capital costs [3]. MEE is the most advanced thermal desalination process for desalting seawater [4].

Compared with the conventional MEE process, MVC is more efficient and economical due to the reuse of heat steam. MVC, which is known to be attractive and competitive for production capacities less than 5,000 m³/d [5], is a thermal-based desalination system that mainly consists of a mechanical compressor, evaporator (one or more) and preheaters. The concept of MVC was first introduced in 1969. Over several decades, experimental research was conducted, and several commercial applications were developed. An early report by Matz and Fisher [6] in 1981 showed that MVC systems have an equal total production cost compared with the RO method. In 1994, more than 200 units with very small capacity were reported by Zimerman [7]. Veza et al. [8] introduced an MVC desalination plant showing good performance and a reliable process that provided water with high plant factors. Kronenberg and Lokiec [9] described the practical commercial application of steam-driven multi-effect distillation plants in dual-purpose (electricity and water production) applications and the latest developments for single-purpose mechanical vapor compression plants. Aybar [10] investigated an MVC system with a single tube model heat exchanger with a 250 t water/d capacity. Bahar et al. [11] described the performance of the system under variable operating conditions.

There are many parameters affecting the performance of MVC systems including the feed temperature, evaporation temperature, compression ratio, feed split between preheaters, intake seawater temperature, intake seawater mass flow rate, and so on. Several papers have been published about optimization design to improve the performance of MVC systems. Al-Juwayhel et al. [12] compared four different types of single-effect evaporator desalination systems. Only the boiling temperature and its difference from the compressed vapor temperature were discussed as affecting MVC system performance. Ettouney [13] presented a comprehensive design model of the single effect MVC process. System performance was discussed as a function of the product flow rate, brine boiling temperature, the temperature difference in the saturated boiling brine and compressed vapor, and length of the evaporator tube. Ibrahim et al. [14] presented a design analysis of a single-effect MVC desalination unit powered by a grid-connected photovoltaic solar system. Dahmardeh et al. [15] researched the MVC system for the treatment of high salinity wastewater. An optimum value of the temperature difference between the condensing vapor and the boiling brine was obtained to target either lower power consumption or heat transfer surface area. Although previous research has been done, discussions about different design parameters of the MVC system are insufficient.

Like other engineering applications, the unit cost of MVC systems should be considered including the total cost of equipment, chemicals, operations, and maintenance divided by the plant capacity. In the past few years, a new approach called thermo-economic analysis was proposed. Nafey et al. [16] developed exergy and thermo-economic mathematical models that presented how to decrease unit costs for an MEE-MVC. Sharaf et al. [17] compared multi-effect distillation and MVC systems through thermo-economic

analysis. Jamil and Zubair [18] focused on the thermo-economic analysis of a single effect MVC desalination system operating with and without brine recirculation. Schwantes et al. [19] conducted a techno-economic comparison of membrane distillation and MVC in a zero liquid discharge application. Elsayed et al. [20] and Jamil and Zubair [21] compared four feed configurations including forwarding feed, backward feed, parallel feed, and parallel/crossfeed in a thermo-economic analysis. However, the effect of design parameters on the system performance is neglected in the aforementioned literature.

To our knowledge, performance is most important to consider when designing an MVC system, which includes studying the parameter optimization effect on the distillate amount and recovery ratio. At the same time, the unit costs of MVC systems should not be neglected. Finding a compromise between good performance (more distillates) and the unit cost is important in MVC system design. In previous works, parameter optimization and economic analyses have not been combined in such research. In this paper, the parameters affecting MVC system performance and economic analysis are both discussed for a single-effect MVC system optimization design.

2. System description

MVC denotes an efficient and energy-saving evaporation technology what consists of preheaters, evaporators, the mechanical compressor, transfer pumps, and so on. The principle of a single-stage MVC is as follows (Fig. 1). Seawater is pumped into the evaporator across two preheaters, and in the process, the seawater temperature and enthalpy are elevated by two preheaters in parallel. In preheater 1, the seawater temperature increases from T_0 to T_1 after absorbing heat from the outlet brine of the evaporator. In preheater 2, the brine exchanges heat with the outlet condensation water of the tubes, and the temperature increases from T_0 to T_2 . After preheating, the heated water joins together and flows into the evaporator, where it is sprayed outside the tubes; part of the water is evaporated. The vapor generated from the solution flows into the mechanical compressor while the pressure and temperature are improved rapidly. The superheated vapor releases the latent heat and sensible heat to the brine outside the tube surface. At the end of the tubes, the vapor changes to saturated water.

3. Mathematical model

3.1. Preheater

Two preheaters warm the feed seawater before it enters the evaporator in the conventional MVC process. The difference between preheater 1 and preheater 2 is the property of the hot fluid. Inside the first preheater is hot brine from the evaporator; inside the second preheater is hot condensation water from the evaporator tubes. Plate heat exchangers and shell-tube heat exchangers are the most common structures. Although plate heat exchangers are preferable and more cost-efficient, we chose a shell-tube type because of its relatively simple manufacturing and adaptability to different operating conditions [22].

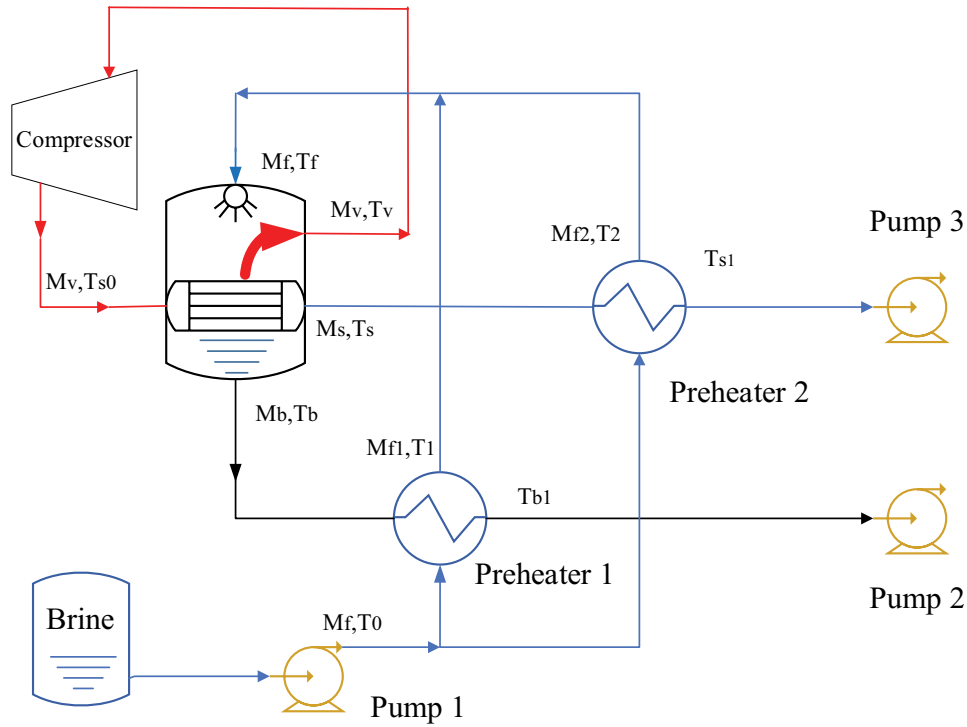


Fig. 1. Schematic of a conventional single-stage MVC process.

The seawater (M_f) is divided into two streams entering each preheater in parallel.

$$M_f = M_{f1} + M_{f2} \quad (1)$$

$$x = \frac{M_{f1}}{M_f} \quad (2)$$

where x is the feed split between preheaters.

The preheater model is based on energy conservation and heat transfer relations.

$$Q_{p,1} = Cp_{b,T_b} (T_b - T_{b1}) M_b = Cp_{f,T_0} (T_1 - T_0) M_{f1} \quad (3)$$

where M_b is the mass flow rate of the outlet brine of the evaporator and M_{f1} is the mass flow rate of feed seawater entering preheater 1. Cp_{b,T_b} and Cp_{f,T_0} are the specific heat capacity of brine and feed seawater, respectively. T_1 and T_0 are the inlet and outlet feedwater temperature, respectively, and T_{b1} and T_b are the inlet and outlet temperature of the brine, respectively.

The heat transfer power $Q_{p,1}$ is calculated from the heat transfer equation:

$$Q_{p,1} = h_{p,1} A_{p,1} \text{LMTD}_{p,1} \quad (4)$$

$\text{LMTD}_{p,1}$ is the logarithmic mean temperature difference, $A_{p,1}$ is the heat transfer area, and $h_{p,1}$ is the overall heat transfer coefficient that is estimated with the following equation [23]:

$$h_{p,1} = 1.7194 + 3.2063 \cdot 10^{-3} T + 1.5971 \cdot 10^{-5} T^2 - 1.9918 \cdot 10^{-7} T^3 \quad (5)$$

$\text{LMTD}_{p,1}$ is calculated according to Eq. (6):

$$\text{LMTD}_{p,1} = \frac{(T_b - T_1) - (T_{b1} - T_0)}{\ln \left(\frac{T_b - T_1}{T_{b1} - T_0} \right)} \quad (6)$$

$$Q_{p,2} = Cp_{s,T_s} (T_s - T_{s1}) M_s = Cp_{f,T_1} (T_2 - T_0) M_{f2} \quad (7)$$

where M_s is the mass flow rate of the condensation water outlet of the tubes and M_{f2} is the mass flow rate of feed seawater entering preheater 2. Cp_{s,T_s} and Cp_{f,T_1} are the specific heat capacity of water and feed seawater, respectively. T_0 and T_2 are the inlet and outlet feed seawater temperature, respectively, and T_s and T_{s1} are the inlet and outlet temperature of the water, respectively.

$Q_{p,2}$ is calculated according to the heat transfer equation:

$$Q_{p,2} = h_{p,2} A_{p,2} \text{LMTD}_{p,2} \quad (8)$$

$A_{p,2}$ is the heat transfer area of preheater 2, and $h_{p,2}$ is the overall heat transfer coefficient that is obtained from Eq. (5).

The logarithmic mean temperature difference $\text{LMTD}_{p,2}$ is calculated as follows:

$$\text{LMTD}_{p,2} = \frac{(T_s - T_2) - (T_{s1} - T_0)}{\ln \left(\frac{T_s - T_2}{T_{s1} - T_0} \right)} \quad (9)$$

Two streams join together and flow into the evaporator. The mixing temperature is obtained as follows:

$$T_f = xT_1 + (1-x)T_2 \quad (10)$$

3.2. Evaporator

Fig. 2 shows a schematic of the thermal process in an evaporator. The feed seawater warmed by two preheaters is sprayed and subsequently drops over the horizontal tube bundle, forming a falling film outside of the tubes. Feed seawater absorbs the heat released from the vapor inside the tube, and then part of it evaporates. Mass and energy equations are proposed:

Mass equation:

$$M_f = M_v + M_b \quad (11)$$

$$M_f \cdot X_0 = M_b \cdot X_1 \quad (12)$$

Energy equation:

$$Q_e = (H_{s0} - H_s)M_s = M_v\lambda_{T_b} + M_f C_p (T_b - T_f) \quad (13)$$

$$M_v = M_s \quad (14)$$

where M_v is the mass flow rate of vapor, M_f and M_b are mentioned above, X_0 and X_1 are the salinity of feed seawater and

brine, respectively, H_{s0} is the enthalpy value of the vapor outlet of the compressor, H_s is the enthalpy value of fresh-water at the end of the tubes, and λ_{T_b} is the latent heat of the vapor.

Additionally, Q_e can be estimated as follows:

$$Q_e = h_e A_e \text{LMTD}_e \quad (15)$$

where A_e is the heat transfer area and h_e is the overall heat transfer coefficient, which can be obtained according to the following equation [24]:

$$h_e = 1961.9 + 12.6T_b - 9.6 \times 10^{-2}T_b^2 + 3.16 \times 10^{-4}T_b^3 \quad (16)$$

The logarithmic mean temperature difference LMTD_e is calculated as follows:

$$\text{LMTD}_e = \frac{(T_{s0} - T_s) - (T_b - T_f)}{\ln\left(\frac{T_{s0} - T_s}{T_b - T_f}\right)} \quad (17)$$

The boiling point elevation (BPE) is related to the rise in the boiling temperature at a given pressure due to the salt concentration.

$$T_v = T_b - \text{BPE} \quad (18)$$

3.3. Mechanical compressor

In an MVC system, the vapor compressor is the major energy consumption device, and its work can be calculated as follows [25]:

$$W_{\text{comp}} = M_v \frac{C_p T_v}{\eta_{\text{comp}}} \left(\alpha^{\left(\frac{\gamma-1}{\gamma}\right)} - 1 \right) \quad (19)$$

where η_{comp} is the thermal efficiency of the compressor, α is the pressure ratio across the compressor, and γ is the isentropic coefficient that is estimated to be 1.3 [13].

$$T_{s0} = T_v \cdot (\alpha)^{(\gamma-1)/\gamma} = T_v \cdot \left(\frac{P_{s0}}{P_v} \right)^{(\gamma-1)/\gamma} \quad (20)$$

where $\gamma = 1/\{1-[8.314/(18 \cdot C_p)](1+X)^2/Y\}$, $X = 0.004256$, and $Y = 1.0011$.

3.4. Transfer pumps

In an MVC system, there are at least three transfer pumps, including a feed pump, a brine pump, and a distillate pump. The pump power can be expressed as follows [18]:

$$W_{\text{pump}} = \frac{V \cdot \Delta P}{\eta_{\text{pump}}} \quad (21)$$

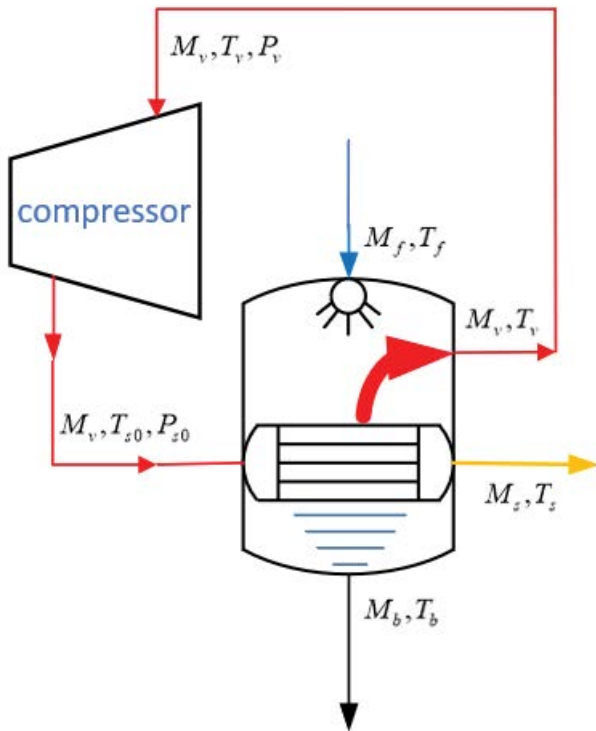


Fig. 2. Schematic of the evaporator integrated with a compressor.

where V is the volume flow rate, ΔP is the pressure difference, and η_{pump} is the thermal efficiency of the transfer pump.

3.5. Recovery ratio

The recovery ratio is an important parameter to measure the distillate efficiency of an MVC system. The heat steam input of an MVC system comes from the recyclable vapor from the evaporator. The recovery ratio (RR) can be calculated as follows [8]:

$$RR = \frac{M_s}{M_f} \quad (22)$$

4. Simulation algorithm

4.1. Parameter input and main assumptions

The required input parameters are defined below:

- Feed seawater temperature ranges from 5°C to 35°C [13].
- Seawater salinity is assumed to be 35,000 ppm.
- Feed seawater flow rate ranges from 10 to 58 kg/s.
- Feed seawater temperature varies from 58°C to 70°C [2].
- Pump efficiency is assumed to be 78% [21].
- Mechanical vapor compressor is assumed to be a centrifugal compressor with an efficiency of 70% and a pressure ratio across the compressor of 1.35 [16,21,26].

An MVC system uses complex processes including many parameters and equations. It is very important to

make some assumptions for conventional analysis. To simplify the model calculations, the main assumptions used in this study are the following:

- Process is assumed to be steady-state, which means modeling does not consider start-up and shutdown, so the variables do not depend on time [2].
- Distillate is salt-free [27].
- Heat losses to the surroundings are neglected because it is assumed that the outer sidewalls of the evaporators and preheaters are well insulated [2].
- Horizontal falling film tubes, steam is turned into saturated water, and the pressure drop is negligible.
- Gas is defined as an ideal gas.
- Minimum temperature difference of the preheater (ΔT) exceeds 2°C.
- Non-equilibrium allowance is neglected [2].

4.2. Computational method and process

PYTHON language is used to model the MVC process. In the Python software, the IAPWS module is used to calculate the physical properties of water-vapor and brine, which is convenient for use in MVC system design.

The computational process is listed in Fig. 3. In the beginning, the parameters T_0 , M_f , α , RR, X_0 are defined and input into the procedure code. By reasonable assumption and calculation, the design parameters are obtained in detail. The reasonable definition of the input parameters is introduced in the next section.

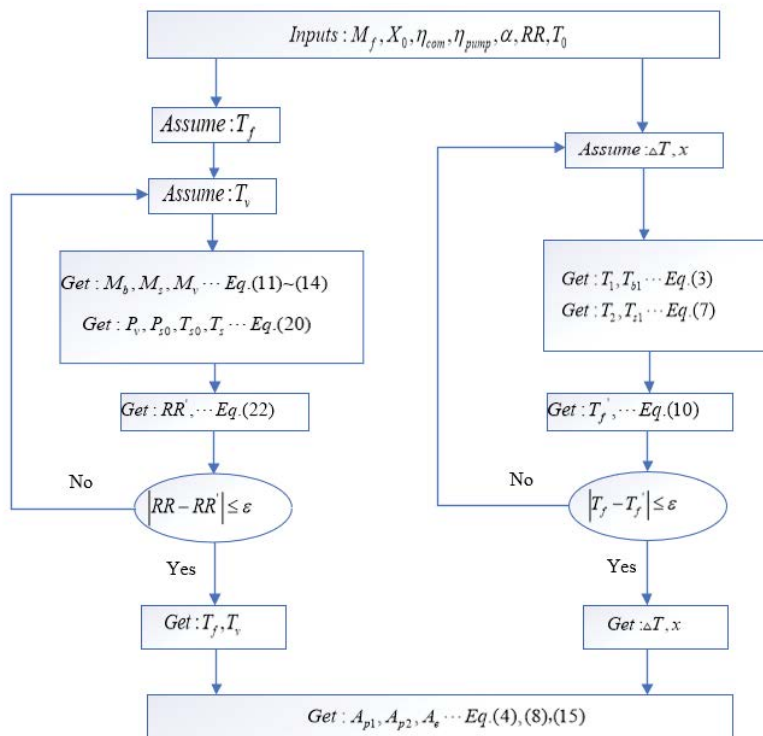


Fig. 3. Computational process in the procedure code.

5. Results and discussion

5.1. Model accuracy verification

For substantiating the accuracy of the simulation methodology and results, the model results were compared with values from Jamil and Zubair [18] and are listed in Table 1.

As is seen in Table 1, the model results fit quite well with those from Jamil and Zubair [18], noting especially that the recovery ratio difference is almost negligible. The biggest relative error of all parameters is the compression ratio, which is still below 6%. This shows that the model in this paper is reliable.

5.2. Effects of the feed seawater temperature (T_f) on the recovery ratio

Seawater is warmed across two preheaters and pumped to the evaporator. In the design of an MVC system, the feed seawater temperature is first defined, and then the parameters of two preheaters are calculated according to the seawater temperature and the hot fluid temperature (the brine temperature and condensation water temperature at the end of the tubes). The effects of the feed seawater temperature variation on MVC system performance are valuable to discuss.

As seen in Fig. 4, the recovery ratio increases with increasing feed seawater temperatures, mainly caused by the difference in the physical property value of the water-vapor at the variation in feed seawater temperature. Eqs. (23) and (24) are the transformations of formula 13. According to Eqs. (23)–(24), the value of the denominator decreases linearly with the feed seawater temperature increase (Fig. 5). More vapor will be generated (M_v) in the evaporator. Consequently, the recovery ratio becomes larger.

The correlation of the recovery ratio and temperature difference between the feedwater temperature and saturation temperature (Δt) is demonstrated in Fig. 4. Under

various temperature differences ($\Delta t = 1$, $\Delta t = 1.5$, $\Delta t = 2$), the larger the temperature difference, the higher is the recovery ratio. This occurs because, as calculated with Eqs. (23)–(24), the temperature difference increase mainly improves the value of the numerator, which increases the amount of vapor produced and the recovery ratio.

$$M_v = \frac{M_f C_p (T_b - T_f)}{H_{s0} - H_s - \lambda_{T_b}} \quad (23)$$

$$RR = \frac{M_v}{M_f} = \frac{C_p (T_b - T_f)}{H_{s0} - H_s - \lambda_{T_b}} \quad (24)$$

5.3. Effects of the feed seawater flow rate

The feed seawater flow rate is an important parameter to consider when measuring plant capacity. Fig. 6 shows that under the special parameters $T_f = 58^\circ\text{C}$, $T_v = 60^\circ\text{C}$, $T_0 = 20^\circ\text{C}$, the distillate production flow rate and recovery ratio change with different feed seawater flow rates (between 10 and 58 kg/s). With the feed seawater flow rate increase, the amount of distillate increases in a linear relation, while the recovery ratio remains constant at approximately 0.75. These results show that feed seawater flow rate only affects plant capacity, not distillate efficiency because the feed seawater flow rate increase leads to more vapor generation. As shown in Eqs. (23)–(24), as the other parameters are constant, the vapor flow rate (M_v) is directly proportional to the feed seawater flow rate (M_f). Therefore, as the feed seawater and vapor flow rate vary simultaneously, the recovery ratio will remain constant.

5.4. Effects of seawater temperature

The seawater temperature does not remain constant throughout the year and often varies with the environment. It is very important to define a suitable seawater temperature when designing an MVC system. Seawater temperature varying from 5°C to 30°C is considered in this study. With constant feed seawater temperature and saturation temperature, the variation in the seawater temperature only affects the preheater area, not the evaporator performance. Under the condition of $T_f = 58^\circ\text{C}$, $T_v = 60^\circ\text{C}$, $M_f = 10$ kg/s, the fluid temperatures at the inlet and outlet of the preheaters are listed in Table 2.

As is shown in Table 2, for meeting the feed temperature requirements when entering the evaporator, with the seawater temperature increase, the cold fluid temperature difference and heat power across the preheater decrease. This results in a decrease in the heat transfer area.

For MVC plant design, low seawater temperature should be considered first, because more heat transfer area and higher heat transfer efficiency are needed in this situation.

5.5. Recovery ratio definition

The recovery ratio is an important parameter that affects MVC plant capacity. Similar to feedwater mass flow,

Table 1
Comparison of values from Jamil and Zubair [18] and the model results

Parameter	Jamil and Zubair [18]	Model results
Intake seawater temperature, $^\circ\text{C}$	21	21
Feed seawater temperature, $^\circ\text{C}$	61	61
Evaporation temperature, $^\circ\text{C}$	63	62.7
Vapour temperature, $^\circ\text{C}$	61.9	61.7
Distillate temperature, $^\circ\text{C}$	67	67
Compressed vapour temperature, $^\circ\text{C}$	81	83
Compression ratio, α	1.21	1.29
Intake seawater salinity, g/kg	40	40
Brine salinity, g/kg	80	85
Feed split ratio between preheaters, x , %	50	53
Feed flow rate, kg/s	26	26
Plant capacity, kg/s	13	13.8
Recovery ratio, RR	0.5	0.53

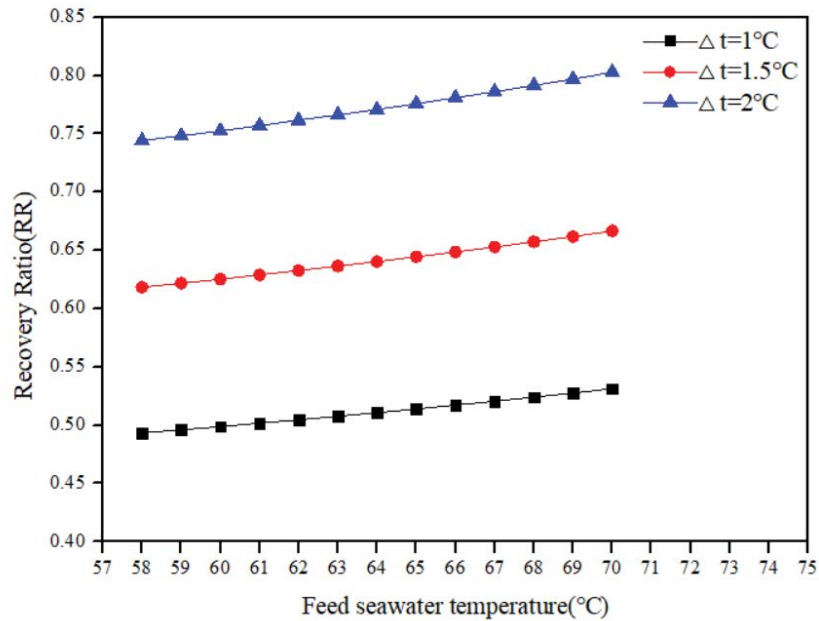


Fig. 4. Recovery ratio with different feed temperatures.

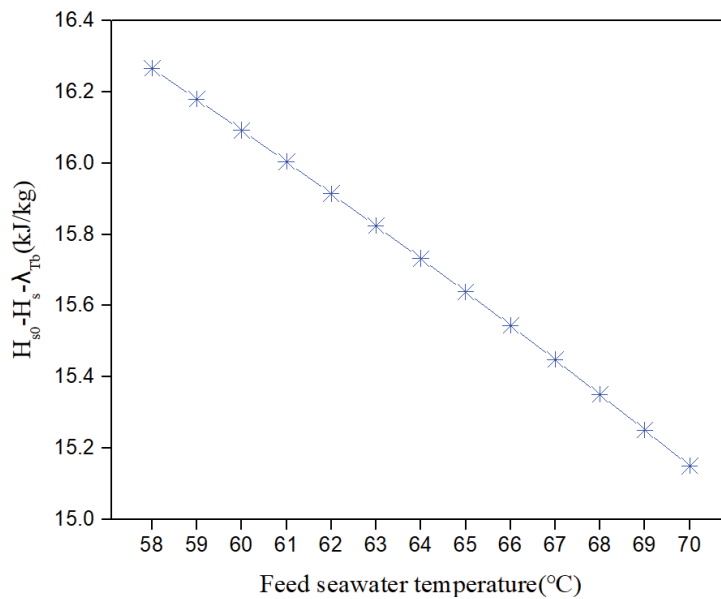


Fig. 5. Physical property value difference of the water-vapor with different feed temperatures.

the greater the recovery ratio, the better is the MVC plant performance. Seawater distillation includes two main processes, concentration, and crystallization. In the concentration process, seawater evaporates from the salinity of 35–250 g/kg [28]. This evaporation often occurs in a brine concentrator that operates on the principle of MVC. The subsequent crystallization step is usually carried out by a forced circulation crystallizer or an evaporation pond before disposing of the solids in a landfill. In the crystallization process, the brine flow state and physical properties change. Therefore, several questions are raised including

those about corrosion-resistance and the calculation equation accuracy. Corrosion-resistant metal alloys and metals such as titanium are used for heat exchange surfaces. Titanium, in particular, has been operationally found to be a very reliable material, resistant to corrosion and erosion at both high salinities and temperatures. However, titanium is too expensive, thus increasing capital costs. We believe that a type of inexpensive material will speed up the development of thermal crystallization. Currently, many calculation equations are used for the concentration process, with such equations including the overall heat transfer coefficient.

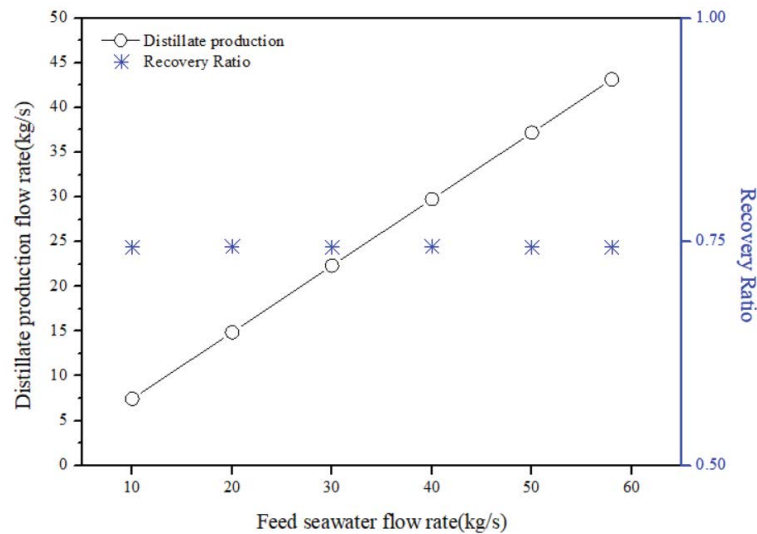


Fig. 6. Distillate production flow rate and recovery ratio under different feed seawater flow rates.

Table 2
Fluid temperatures at the inlet and outlet of the preheaters

	Parameter					
Seawater temperature, $T_{0'}$ °C	5	10	15	20	30	35
Preheater 1						
Outlet temperature, cold, $T_{1'}$ °C	52.3	52.5	52.5	52.7	52.9	53.1
Inlet temperature, hot, $T_{2'}$ °C	61	61	61	61	61	61
Outlet temperature, hot, $T_{3'}$ °C	13	18	23	27.8	37.6	42.6
Total transfer heat area, m^2	22.8	22.6	22.4	22.2	21.8	21.6
Preheater 2						
Outlet temperature, cold, $T_{2'}$ °C	59.7	59.6	59.6	59.6	59.5	59.4
Inlet temperature, hot, $T_{3'}$ °C	66.6	66.6	66.6	66.6	66.6	66.6
Outlet temperature, hot, $T_{4'}$ °C	13	18	23	27.8	37.6	42.6
Total transfer heat area, m^2	22.8	22.6	22.4	22.2	21.8	21.6

As mentioned above, only the concentration process is considered in this paper. By calculation, the recovery ratio cannot exceed 0.86. For simplified discussion, in this paper, the recovery ratio is set to vary over a range of 0.5–0.86.

5.6. Economic analysis

MVC plants involve several kinds of costs and revenues over a long period during their operation life, including initial capital cost, running cost, labor and chemical cost, etc.

In most previous studies [29,30], a parameter called the simplified cost of water (SCOW) is used to define the initial capital cost, which can be calculated using Eq. (25) as follows:

$$SCOW = \frac{(I_0 \cdot \phi) + C_t}{M_w} \quad (25)$$

where the amortization factor (ϕ) is defined as follows in Eq. (26):

$$\phi = \frac{i(1+i)^n}{(1+i)^n - 1} \quad (26)$$

where i is the interest rate and n is the number of years of the economic life of the system, taken as 0.05 and 20, respectively [29]. By calculation, ϕ is 0.85.

In Eq. (26), it is assumed that every year (from year 1 to year n) the desalination plant produces the same amount of water (M_w) and has the same running cost (C_t).

Capital cost (I_0) contains several factors, such as equipment, materials, pumps, land, initial design, permitting and so on, which can be calculated in detail during the design phase. The main correlations for the capital cost are listed in Table 3.

Running cost (C_t) is the annual operating cost that mainly includes the cost of energy (heat and electricity), seawater

Table 3
Main equations for capital cost calculation

Component	Equation	Parameter range	Reference
Preheater	$Z_{pre} = 1,000(12.86 + A_{pre}^{0.8})$	N/A	[31]
Evaporator	$Z_{evap} = C \cdot (A_e)^\gamma$	$C = 300 \text{ €/m}^2, \gamma = 0.95$	[32]
Compressor	$Z_{comp} = 7,364m_v \cdot \alpha \cdot e^{0.7}$	$10 \leq m_v \leq 455, 1.1 \leq \alpha \leq 2$ $2.3 \leq e \leq 11.5$ $e = \frac{\eta_{comp}}{1 - \eta_{comp}}$	[33]
Pump	$Z_{pump} = 13.92m_{water} \Delta p^{0.55} e^{1.05}$	$2 \leq m_{water} \leq 32$ $100 \leq \Delta p \leq 6,200$ $1.8 \leq e \leq 9$ $e = \frac{\eta_{pump}}{1 - \eta_{pump}}$	[18]

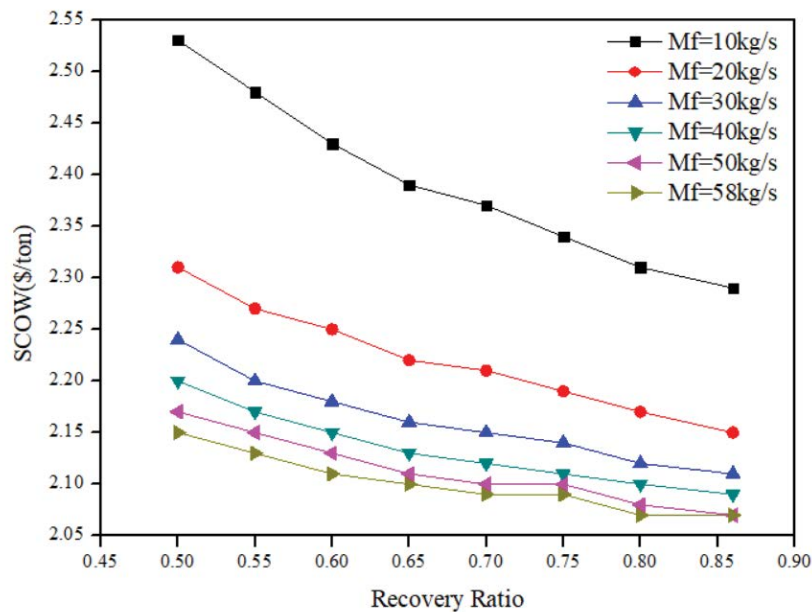


Fig. 7. SCOW (\$/ton) of different mass flow ratios of feed water under different recovery ratio conditions.

pre-treatment chemicals, labor, maintenance, and management. The following assumptions are made in this study: unit electricity cost is 0.07 \$/kWh; chemical consumption per ton of seawater is 0.005 kg/ton, and the unit chemical cost is 1.46 \$/kg; the yearly operator salary is 6,000 \$/operator with the plant using 6 operating workers; the annual maintenance cost is estimated as 1.5% of the capital cost; the annual management cost is estimated as 20% of the labor cost [17,34].

Electricity costs (EC) can be calculated as follows in Eq. (27):

$$EC = 365 \times 24 \times UEP \times SP \times M_w \tag{27}$$

where UEP is the unit electricity price 0.07 \$/kWh, SP is the sum of the pump power and compressor power consumption in kWh/m³, and M_w is the amount of fluid.

The economic analysis is focused on comparisons of the initial capital cost of different plant capacities. Other parameters are defined as follows: T_f = 70°C, T₀ = 5°C. The SCOW (\$/ton) of different mass flow ratios of feed seawater under different recovery ratio conditions is illustrated in Fig. 7.

It is found that with increasing feed seawater flow rate and recovery ratio, the SCOW shows a decreasing trend from 2.37 to 2.03 (\$/ton). In the beginning, the SCOW declines quickly. With M_f exceeding 40 kg/s, the SCOW changes slowly.

At the same seawater flow rate, the SCOW decreases with an increase in the recovery ratio. This is because the distillate production increase leads to a decrease in the initial capital cost per unit flow rate.

6. Conclusions

In this paper, the optimization design and economic analysis of a single-effect MVC distillation system are investigated. The parameters including the RR, seawater temperature (T_0), seawater flow rate (M_p), feed seawater temperature (T_f), and temperature difference in the feed seawater and saturation temperature (Δt) are discussed to improve the MVC system performance. An economic analysis is also presented by comparing the SCOW value at various plant capacities and recovery ratios.

The results indicate that the recovery ratio increases with an increase in the feed seawater temperature and the temperature difference in the feed temperature and saturation temperature. With the feed seawater flow rate increase, the amount of the distillate becomes greater, and the recovery ratio remains constant. The seawater temperature variable only affects the preheater area, not the performance of the evaporator. With increased seawater temperature, the preheater area decreases. Although the difference in the preheater area is small, the seawater temperature should not be neglected. To design an MVC system, a low seawater temperature condition is considered first.

The economic analysis shows that with an increase in the feed seawater flow rate and the recovery ratio, SCOW decreased. Only considering the costs, the MVC plant capacity and the recovery ratio should be as large as possible.

Symbols

T_0	—	Seawater temperature, °C
T_1	—	Outlet feed water temperature of preheater 1, °C
T_f	—	Feed seawater temperature, °C
T_b	—	Brine temperature, °C
T_{b1}	—	Outlet brine temperature of preheater 1, °C
T_s	—	Outlet condensed water temperature of the tubes, °C
T_{s1}	—	Outlet water temperature of preheater 2, °C
T_v	—	Saturation temperature, °C
T_{s0}	—	Outlet vapor temperature of the compressor, °C
Δt	—	The temperature difference between the feed seawater temperature and saturation temperature, °C
M_f	—	Feed seawater mass flow rate, kg/s
M_b	—	Brine mass flow rate, kg/s
M_v	—	Vapor mass flow rate, kg/s
M_s	—	Outlet condensed water mass flow rate of the tubes, kg/s
C_p	—	Special heat capacity, kJ/kg K
H_{s0}	—	Enthalpy value of the outlet vapor of the compressor, kJ/kg

H_s	—	Enthalpy value of the outlet vapor of the tubes, kJ/kg
A_e	—	Evaporator heat area, m ²
$A_{p,1}$	—	Preheater 1 area, m ²
$A_{p,2}$	—	Preheater 2 area, m ²
W_{comp}	—	Power of the compressor, KW
BPE	—	Boiling point elevation, °C
RR	—	Recovery ratio
LMTD	—	Logarithmic mean temperature difference
Q	—	Special heat consumption, kW
h	—	Heat transfer coefficient, W/m ² K
X	—	Salt mass fraction, g/kg
SCOW	—	Simplified cost of water, \$/ton
I_0	—	Capital cost, \$
C_t	—	Running cost, \$

Greek

α	—	Pressure ratio across the compressor
γ	—	Isentropic coefficient of the compressor
η_{comp}	—	Thermal efficiency of the compressor
η_{pump}	—	Thermal efficiency of the transfer pump

Subscripts

$p,1$	—	Preheater 1
$p,2$	—	Preheater 2
b	—	Brine
e	—	Evaporator
f	—	Feed
v	—	Vapor

References

- [1] D. Saldivia, C. Rosales, R. Barraza, L. Cornejo, Computational analysis for a multi-effect distillation (MED) plant driven by solar energy in Chile, *Renewable Energy*, 132 (2019) 206–220.
- [2] I.S. Al-Mutaz, I. Wazeer, Comparative performance evaluation of conventional multi-effect evaporation desalination processes, *Appl. Therm. Eng.*, 73 (2014) 1192–11201.
- [3] B. Han, Z.L. Liu, H.Q. Wu, Y.X. Li, Experimental study on a new method for improving the performance of thermal vapor compressors for multi-effect distillation desalination systems, *Desalination*, 344 (2014) 391–395.
- [4] R.K. Kamali, S. Mohebinia, Experience of design and optimization of multi-effects desalination systems in Iran, *Desalination*, 222 (2008) 639–645.
- [5] R. Borsani, S. Rebagliati, Fundamentals and costing of MSF desalination plants and comparison with other technologies, *Desalination*, 182 (2005) 29–37.
- [6] R. Matz, U. Fisher, A comparison of the relative economics of sea water desalination by vapour compression and reverse osmosis for small to medium capacity plants, *Desalination*, 36 (1981) 137–151.
- [7] Z. Zimmerman, Development of large capacity high efficiency mechanical vapor compression (MVC) units, *Desalination*, 96 (1994) 51–58.
- [8] J.M. Veza, Mechanical vapour compression desalination plants – a case study, *Desalination*, 101 (1995) 1–10.
- [9] G. Kronenberg, F. Lokiec, Low-temperature distillation processes in single- and dual-purpose plants, *Desalination*, 136 (2001) 189–197.
- [10] H.S. Aybar, Analysis of a mechanical vapor compression desalination system, *Desalination*, 142 (2002) 181–186.
- [11] R. Bahar, M.N.A. Hawlader, L.S. Woei, Performance evaluation of a mechanical vapor compression desalination system, *Desalination*, 166 (2004) 123–127.

- [12] F. Al-Juwayhel, H. El-Dessouky, H. Ettouney, Analysis of single-effect evaporator desalination systems combined with vapor compression heat pumps, *Desalination*, 114 (1997) 253–275.
- [13] H. Ettouney, Design of single-effect mechanical vapor compression, *Desalination*, 190 (2006) 1–15.
- [14] M. Ibrahim, A. Arbaoui, Y. Aoura, Design analysis of MVC desalination unit powered by a grid connected photovoltaic system, *Energy Procedia*, 139 (2017) 524–529.
- [15] H. Dahmardeh, H.A. Akhlaghi Amiri, S.M. Nowee, Evaluation of mechanical vapor recompression crystallization process for treatment of high salinity wastewater, *Chem. Eng. Process. Process Intensif.*, 145 (2019) 107682.
- [16] A.S. Nafey, H.E.S. Fath, A.A. Mabrouk, Thermo-economic design of a multi-effect evaporation mechanical vapor compression (MEE–MVC) desalination process, *Desalination*, 230 (2008) 1–15.
- [17] M.A. Sharaf, A.S. Nafey, L. García-Rodríguez, Thermo-economic analysis of solar thermal power cycles assisted MED-VC (multi effect distillation-vapor compression) desalination processes, *Energy*, 36 (2011) 2753–2764.
- [18] M.A. Jamil, S.M. Zubair, On thermo-economic analysis of a single-effect mechanical vapor compression desalination system, *Desalination*, 420 (2017) 292–307.
- [19] R. Schwantes, K. Chavan, D. Winter, C. Felsmann, J. Pfafferoth, Techno-economic comparison of membrane distillation and MVC in a zero liquid discharge application, *Desalination*, 428 (2018) 50–68.
- [20] M.L. Elsayed, O. Mesalhy, R.H. Mohammed, L.C. Chow, Performance modeling of MED-MVC systems: exergy-economic analysis, *Energy*, 166 (2019) 552–568.
- [21] M.A. Jamil, S.M. Zubair, Effect of feed flow arrangement and number of evaporators on the performance of multi-effect mechanical vapor compression desalination systems, *Desalination*, 429 (2018) 76–87.
- [22] V.K. Patel, R.V. Rao, Design optimization of shell-and-tube heat exchanger using particle swarm optimization technique, *Appl. Therm. Eng.*, 30 (2010) 1417–1425.
- [23] P. Palenzuela, A.S. Hassan, G. Zaragoza, D.C. Alarcón-Padilla, Steady state model for multi-effect distillation case study: Plataforma Solar de Almería MED pilot plant, *Desalination*, 337 (2014) 31–42.
- [24] H. El-Dessouky, I. Alatiqi, S. Bingulac, H. Ettouney, Steady-state analysis of the multiple effect evaporation desalination process, *Chem. Eng. Technol.*, 21 (1998) 437–451.
- [25] G.P. Thiel, E.W. Tow, L.D. Banchik, H.W. Chung, J.H. Lienhard V, Energy consumption in desalinating produced water from shale oil and gas extraction, *Desalination*, 366 (2015) 94–112.
- [26] M.N. Labib, S.S. Kim, D. Choi, T. Utomo, H. Chung, H. Jeong, Numerical investigation of the effect of inlet skew angle on the performance of mechanical vapor compressor, *Desalination*, 284 (2012) 66–76.
- [27] M.H. Khademi, M.R. Rahimpour, A. Jahanmiri, Simulation and optimization of a six-effect evaporator in a desalination process, *Chem. Eng. Process. Process Intensif.*, 48 (2009) 339–347.
- [28] H.W. Chung, K.G. Nayar, J. Swaminathan, K.M. Chehayeb, J.H. Lienhard V, Thermodynamic analysis of brine management methods: Zero-discharge desalination and salinity-gradient power production, *Desalination*, 404 (2017) 291–303.
- [29] A.M. El-Nashar, Economics of small solar-assisted multiple-effect stack distillation plants, *Desalination*, 130 (2000) 201–215.
- [30] M. Papapetrou, A. Cipollina, U. La Commare, G. Micale, G. Zaragoza, G. Kosmadakis, Assessment of methodologies and data used to calculate desalination costs, *Desalination*, 419 (2017) 8–19.
- [31] W. El-Mudir, M. El-Bousiffi, S. Al-Hengari, Performance evaluation of a small size TVC desalination plant, *Desalination*, 165 (2004) 269–279.
- [32] A. Piacentino, Application of advanced thermodynamics, thermo-economics and exergy costing to a multiple effect distillation plant: in-depth analysis of cost formation process, *Desalination*, 371 (2015) 88–103.
- [33] Y.M. El-Sayed, Designing desalination systems for higher productivity, *Desalination*, 134 (2001) 129–158.
- [34] Y. Wang, N. Lior, Thermo-economic analysis of a low-temperature multi-effect thermal desalination system coupled with an absorption heat pump, *Energy*, 36 (2011) 3878–3887.